Enhanced wide range monotonic piezoresistivity, reliability of Ketjenblack/deproteinized natural rubber nanocomposite, and its biomedical application

Article *in* Journal of Applied Polymer Science · February 2017

DOI: 10.1002/app.44981

CITATIONS
11

READS
322

7 authors, including:

Dr Madhanagopal Jagannathan
Asian Institute of Medicine, Science and Technology
12 PUBLICATIONS **113** CITATIONS
SEE PROFILE

Om Prakash Singh
Tyndall National Institute
41 PUBLICATIONS **168** CITATIONS
SEE PROFILE

Sornambikai Sundaram
Bharathiar University
21 PUBLICATIONS **358** CITATIONS
SEE PROFILE

Kathiresan Sathasivam
Asian Institute of Medicine, Science and Technology
85 PUBLICATIONS **1,823** CITATIONS
SEE PROFILE

Journal of Applied Polymer Science

Enhanced wide range monotonic piezoresistivity, reliability of Ketjenblack/deproteinized natural rubber nanocomposite, and its biomedical application

Jagannathan Madhanagopal,[1] Om Prakash Singh,[2] Sundaram Sornambikai,[1] Abdul Hafidz Omar,[3] Kathiresan V. Sathasivam,[4] S. J. Fatihhi,[5] Mohammed Rafiq Abdul Kadir[1]

[1]Medical Devices and Technology Group (MEDITEG), Universiti Teknologi Malaysia (UTM), 81310 Skudai, Johor Bahru, Johor, Malaysia

[2]Bio-signal Processing Group (BSP), Universiti Teknologi Malaysia (UTM), 81310 Skudai, Johor Bahru, Johor, Malaysia

[3]Institute of Human Centered Engineering (IHCE), Universiti Teknologi Malaysia (UTM), 81310 Skudai, Johor Bahru, Johor, Malaysia

[4]Faculty of Applied Sciences, AIMST University, Semeling campus, Bedong, Kedah, Malaysia

[5]Malaysian Institute of Industrial Technology, Universiti Kuala Lumpur, Bandar Seri Alam, Johor, Malaysia

Correspondence to: M. R. A. Kadir (E-mail: rafiq@biomedical.utm.my)

ABSTRACT: Piezoresistive behavior of 6 to 9 wt % Ketjenblack reinforced deproteinized natural rubber (KB/DPNR) nanocomposite developed by two-roll mill was studied under compressive pressure (0 to 12.54 MPa). The 6 wt % KB/DPNR exhibited monotonic piezoresistivity, the highest electrical resistance change (485%), remarkable reversibility and minimal hysteresis. Furthermore, a good sensitivity (S) = 1.1 MPa^{-1} for 0.25 to 2.49 MPa, high test–retest reliability (intraclass correlation co-efficient, ICC = 0.99) under 0 to 2.49 MPa for three repetitions conducted at an interval of 24 h and excellent repeatability (standard deviation, SD = 4.8%) to a swing of 6.25 MPa for 50 cyclic compression were achieved. Homogeneous dispersion and high aspect ratio of KB and higher chemical linkage (due to double cross linking agents) between KB and DPNR may be responsible for the enhanced piezoresistivity. For practical application, the KB/DPNR was interfaced with the microcontroller through a bridge rectifier via custom-built Simulink and successfully monitored finger pressure in real time during bone movement on human. © 2017 Wiley Periodicals, Inc. J. Appl. Polym. Sci. **2017**, *134*, 44981.

KEYWORDS: deproteinized natural rubber; high pressure sensitivity; Ketjenblack; monotonic piezoresistivity

Received 28 November 2016; accepted 6 February 2017
DOI: 10.1002/app.44981

INTRODUCTION

Electrically conductive nanocomposites consisting of nanocarbon reinforced polymers possessing excellent piezoresistive properties have attracted remarkable research interest for the development of biomedical, sports, aerospace, and automobile industries due to their low-cost, ease of preparation, flexibility, light-weight, and good sensitivity (S).[1–9] For instance, recently, single-walled carbon nanotube (SWCNT)/hydrogel spheres composite reported by Tai *et al.*,[10] sensitive graphene oxide developed by Tian *et al.*,[11] graphene rubber nanocomposite reported by Boland *et al.*[12] have successfully utilized their material for monitoring finger movement, wrist and carotid pulse, finger pressure, breathing pattern and muscle motion during speech. All these above-mentioned works were reported with excellent reproducibility, low hysteresis and good sensitivity under subtle (1 Pa–1 kPa), low (1–10 kPa), and medium (10–100 kPa) pressure sensing regime. However, when large pressure is applied (e.g., 0.5–10 MPa), the carbon nanotube, graphite, and graphene-based composites failed to show high pressure sensitivity, monotonic behavior, remarkable repeatability, and low hysteresis at the same time[2,13] which warrants additional research in high pressure sensing regime. Furthermore, the material possessing monotonic piezoresistivity are highly preferred for sensing application due to easiness of calibrating the sensor and to avoid the complexity of signal processing.[14]

Few researches have been conducted on carbon based polymer composites to achieve the monotonic piezoresistivity in the high compressive pressure sensing range.[2,14–16] For example, 26 vol % carbon black/silicone rubber (CB/SR) developed using solution mixing method under 1 MPa reported by Cai *et al.*[2]

Additional Supporting Information may be found in the online version of this article.

exhibited negative piezoresisitve co-efficient of resistance (NPCR) below 0.6 MPa and positive piezoresistive co-efficient of resistance (PPCR) beyond 0.6 MPa. However, they reported that by incorporating graphene nanoplatelets into the CB/SR, the material revealed monotonicity until 1 MPa. In another research, Ketjenblack(KB)/SR composite treated with NaCl to develop porosity by Yoshimuraa *et al.*[15] showed monotonic piezoresistivity until 1.8 MPa for porous composite than the nonporous composite. Likewise, Wang *et al.*[14] developed 14 vol % and 26 vol % multiwalled carbon nanotube (MWCNT)/SR by solution mixing method and examined under compressive stress (0–2 MPa) revealed the 14 vol % MWCNT with monotonic PPCR behavior than the 26 vol % MWCNT (exhibited both PPCR and NPCR in the investigated range), which favours the 14 vol % MWCNT/silicone rubber composite, suitable for sensor applications. Whereas, the 7 vol % graphite/polyethylene composite (0–40 MPa) developed by Lu *et al.*[16] using two-roll mill without cross linking agents also exhibited NPCR up to 7 MPa and PPCR beyond that. In all these works, higher amount of filler content was utilized with time consuming composite preparation duration (3 days to 14 days), no report on sensitivity and reliability, and cost-effectiveness of CNT, graphite, graphene is also questionable. Therefore, developing a suitable low-cost composite with low-filler content by fast and simple industrial standard preparation method and possessing a wide range of monotonic piezoresistivity, excellent sensitivity, test–retest reliability, and repeatability for high pressure sensing applications is still highly demanding research.

Of late, a new class of natural rubber, deproteinized natural rubber (DPNR) was developed and is widely used in medical and pharmaceutical applications such as trans-dermal drug delivery, gloves, plasters, and catheters.[17–19] This protein removed natural rubber may be an ideal choice as a pressure sensing matrix, due to its high softness compared to other rubbers including SR. In addition, the DPNR possess excellent mechanical properties, impermeable to liquids and gases, easiness of forming films, and nonallergic nature to the humans even at direct contact during testing than other rubbers.[18,19] Besides, to the best of our knowledge, the piezoresistive responses of nanocarbon/DPNR composite in the wide range of compressive load have rarely been explored until now. In this work, we report a KB/DPNR composite with double cross linking agents [dicumyl peroxide (DCP) and trimethylolpropane trimethacrylate (SR 350)] and its detailed study on the piezoresistive behavior, sensitivity, test–retest reliability and repeatability of the newly developed KB/DPNR nanocomposite under compressive pressure of 0 to 12.54 MPa. Furthermore, the developed nanocarbon/DPNR composite was successfully integrated with the microcontroller controlled by custom-built Simulink program through a bridge rectifier for real-time monitoring finger pressure during accessory movement of bone in real-time situations.

EXPERIMENTAL

Materials

Ketjenblack EC 600JD (DBP absorption (495 cm^3/100 g), BET surface area (1270 m^2/g) and primary particle radius 34 nm) and silver paste were purchased from the Lion Corporation, Japan, and Sigma Aldrich, Malaysia, respectively. The deproteinized natural rubber (DPNR) and two cross linking agents (SR 350 and DCP) were donated by the Malaysian Rubber Board and Sakura Rubber Sdn.Bhd, Malaysia, respectively.

Table I. Ingredients of KB/DPNR Nanocomposites

		wt % of Ingredients		
Sample no.	DPNR (phr[a])	KB	SR350	DCP
1	100	3	1.07	1.00
2	100	4	1.07	1.00
3	100	5	1.07	1.00
4	100	6	1.07	1.00
5	100	7	1.07	1.00
6	100	8	1.07	1.00
7	100	9	1.07	1.00

[a] Part per hundred parts of DPNR by weight.

Preparation of KB/DPNR Nanocomposite

The KB (3–9 wt %) of the DPNR and cross linking agents (DCP and SR 350) were hand mixed for 5 min. Then, the hand mixed compounds were incorporated in a two-roll mill and rotated at a speed of 200 rpm and 10 successive mixing were carried out for better homogenous dispersion of KB into the DPNR matrix. Finally, the roll milled mixture was compounded with a hot press at 160 °C under 3000 lbs pressure for 10 min and dried at room temperature to obtain a KB/DPNR nanocomposite sheet with dimension of 150 mm × 150 mm × 1 mm. The size of the sheet can be tuned as per user requirement by choosing an appropriate mould. The amount of the ingredients used to prepare different wt % of KB/DPNR nanocomposite are given in Table I. A portion of KB/DPNR was cut from the centre of the sheet with the following physical dimensions (50 × 40 × 1 mm) for further studies.

Physical and Electrical Characterization

Field emission scanning electron microscopy (FESEM) and attenuated total internal reflection mode—Fourier transform infrared spectroscopy (ATR-FTIR) using a Hitachi SU8020 (Japan) and Nicolet FTIR spectrophotometer model iD5 (USA), respectively, were carried out to observe the surface morphology of the optimal KB/DPNR and the functional group interactions between the KB and DPNR. The electrical characteristics of the KB/DPNR were studied by two-point techniques with thin copper wires glued using a silver paste and cured at 60 °C for 3 h. In addition, an adhesive copper tape was attached over the dried silver paste for better contact of copper wire with the KB/DPNR. Finally, the KB/DPNR nanocomposite of length between electrodes ($L = 20$ mm), width ($w = 40$ mm), and thickness ($t = 1$ mm) were utilized for electrical characterization. The electrical resistance (R) of the KB/DPNR was directly measured using GwInstek multimeter (8251A) and plugged into the formula, as given below to calculate the electrical conductivity (σ) for all the developed nanocomposites.[14,20]

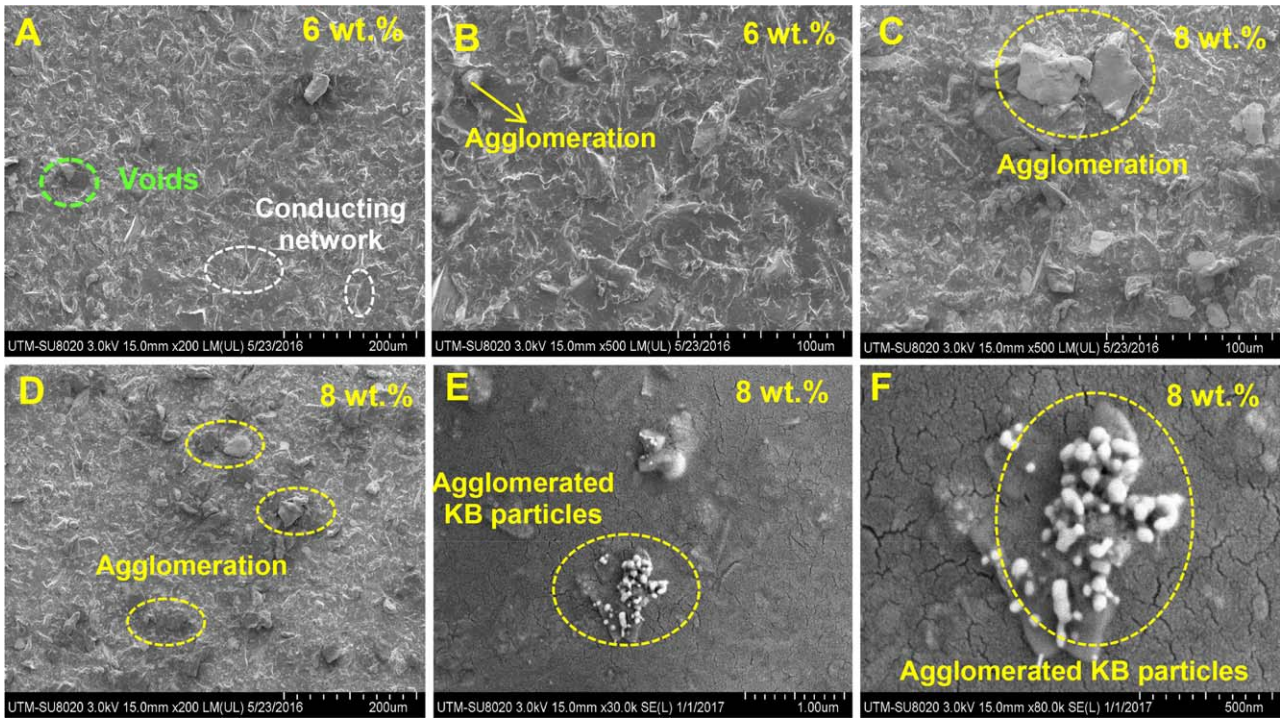

Figure 1. FESEM images of 6 and 8 wt % KB/DPNR nanocomposite (A–D) under different magnifications and the enlarged portion of the agglomerated KB nanoparticles (E,F). [Color figure can be viewed at wileyonlinelibrary.com]

$$\sigma = \left(\frac{1}{\rho}\right) = \left(\frac{1}{R}\right)\left(\frac{L}{A}\right) \quad (1)$$

where ρ, L, R, and A are the electrical resistance, distance between the electrodes, measured resistance and cross-sectional area of KB/DPNR, respectively. The calculated electrical conductivity is presented in the Supporting Information Table S1.

Piezoresistivity Studies

First, the KB/DPNR was glued to acrylic sheets (60 × 60 × 2 mm) and then subjected to compressive testing. To study the piezoresistive response of the KB/DPNR, different controlled compressive loads were applied between 0 and 12.54 MPa at a strain rate of 0.5 mm min^{-1} using 5 kN load cell, Universal tensile testing machine (Instron 5982). To examine the reproducibility of the piezoresistive performance of KB/DPNR composite, the cyclic compressions were carried out with an applied pressure of 6.25 MPa for 50 cycles for the 6 wt % KB/DPNR and 10 cycles for 7 to 9 wt % of KB/DPNR composites. The test–retest reliability of the KB/DPNR performance was studied under applied pressure of 0 to 2.49 MPa for three times at an interval of 24 h. The resistance change during compression was recorded directly by a multimeter. The graphs are plotted for the ratio of change in resistance to original resistance ($\Delta R/R_0$) against time and pressure.

RESULTS AND DISCUSSION

Morphology and Interaction of KB/DPNR

The FESEM images for the surface morphology analysis of 6 and 8 wt % KB within the DPNR matrix at two different magnifications are shown in Figure 1(A–F) for comparison purpose. The morphology of the nanocomposites revealed that 6 wt % KB exhibits homogeneously dispersed KB in addition to conductive network formation between the KB and DPNR as shown in Figure 1(A,B). Besides, very low agglomeration of KB is also noticed for 6 wt % compared to higher number of agglomerations seen for the 8 wt % as shown in Figure 1(C,D), in agreement with the earlier literature.[21] The agglomeration region of 8 wt % is focussed at higher magnification (1 μm and 500 nm) revealed the cluster of spherical KB nanoparticles present within the DPNR as seen in Figure 1(E,F). The FESEM images of 3, 4, 5, 7, and 9 wt % KB/DPNR composites are given in the Supporting Information Figures S1 and S2 at different magnifications. From Supporting Information Figure S1(A–F), good dispersion and more number of voids are noticed for 3 and 4 wt % KB, whereas the 5 wt % of KB also showed a good dispersion with minimal agglomerated surface and less number of voids compared to the 3 and 4 wt %. Furthermore, the FESEM images of 7 [Supporting Information Figure S2(A,B)], 8 [Figure 1(C,D)], and 9 [Supporting Information Figure S2(C,D)] wt % exhibited poorly dispersed KB than those observed for 3 to 6 wt %. These results indicates that the KB/DPNR nanocomposite developed by two-roll mill technique in this study with lower filler content tends to higher dispersion compared to higher filler content.

To study the functional group interactions involved in the KB/DPNR nanocomposite, FTIR was carried out using ATR mode for the composite [Figure 2(A; b)] in comparison with the control DPNR [Figure 2(A; a)] and KB [Figure 2(A; c)]. The ATR-FTIR spectrum of the nanocomposite showed the characteristic =CH stretching at 3048 cm^{-1} for the isoprene functional

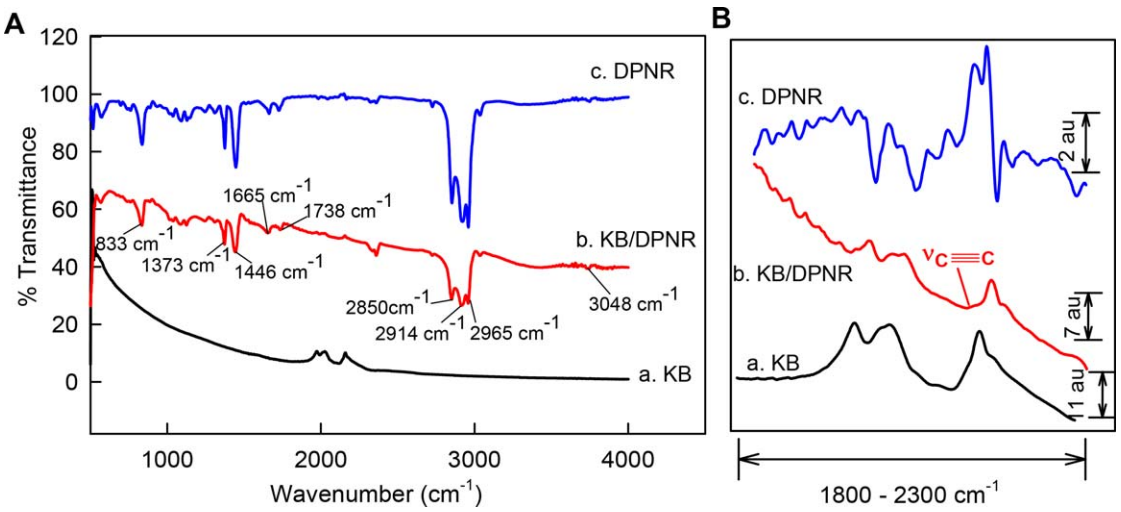

Figure 2. (A) Comparison ATR-FTIR spectra of (a) KB, (b) KB/DPNR nanocomposite and (c) DPNR in between 400 and 4000 cm^{-1}. (B) The enlarged spectra of (a) KB, (b) KB/DPNR nanocomposite and (c) DPNR in between 1800 and 2300 cm^{-1}. [Color figure can be viewed at wileyonlinelibrary.com]

groups, C−H stretching at 2965 cm^{-1} of CH_3, 2914 cm^{-1} of CH_2, and 2850 cm^{-1} for combined CH_3 and CH_2 bonds, respectively, C═N stretching at 1665 cm^{-1}, C−H bending at 1446 cm^{-1} and 1373 cm^{-1} for CH_3 and CH_2 respectively, C═CH wagging at 833 cm^{-1} and C═O stretching at 1738 cm^{-1} which represents the characteristic DPNR spectral bands, in agreement with the earlier literature.[17] Furthermore, the enlarged ATR-FTIR spectrum shown in the Figure 2(B; b) of KB/DPNR in the range of 1800 to 2300 cm^{-1} revealed the presence of C≡C stretching absorptions[22] between 2050 and 2200 cm^{-1} with reduced intensity and slight shift in the transmittance values from those present in the control KB [Figure 2(B; c)]. The C≡C bond has the highest bond energy of 835 KJ mol^{-1} belonging to an σ and two π bonds compared to other bonds involved in the composite which indicates enhanced chemical linkage and requires greater force to break these stronger bonds for any material.[23] All these observations clearly indicate that the bond formation is strong in the KB/DPNR composite which may need more applied compressive loads to break the strong bonds of the proposed composite in this study.

Monotonic Piezoresistive Behaviour of KB/DPNR Nanocomposite

To study the piezoresistive responses of KB/DPNR nanocomposite, 0 to 12.54 MPa compressive pressure were applied to all the composites (6 wt % until 9 wt % KB). The 5 wt % KB/DPNR was not subjected to piezoresistivity testing due to unstable electrical resistance (72.37 ± 1.60 MΩ) under zero load conditions and for <5 wt % KB/DPNR, the electrical resistance was out of range of the multimeter. During compressive loading, all the KB/DPNR composites showed a trend increase in resistance to the applied pressure throughout the investigated range. The relationship between $\Delta R/R_0$ and applied pressure for the KB/DPNR composites with different KB loadings are shown in Figure 3(A). The 6 wt % KB showed $\Delta R/R_0 = 4.85$ (485%) compared to other composites with the following values; 7 wt % (1.2), 8 wt % (0.2), and 9 wt % (0.04), respectively. The

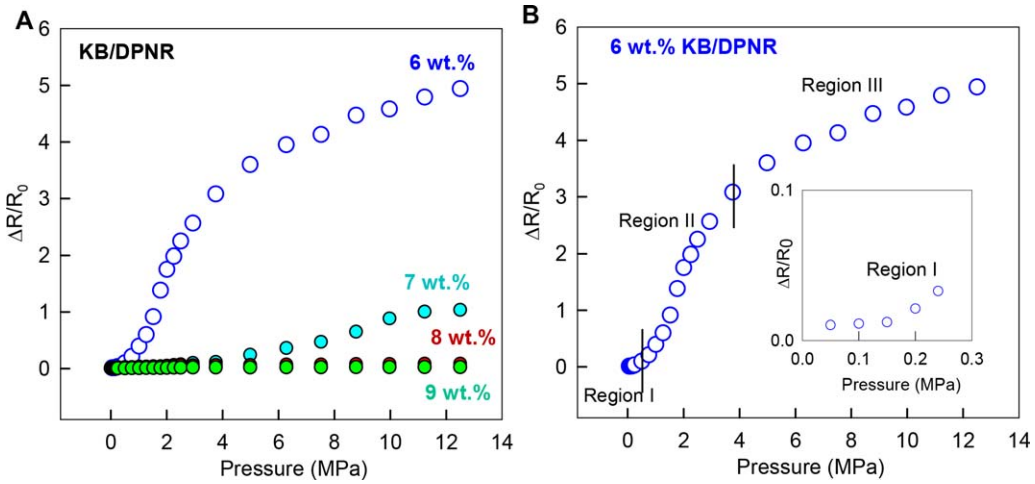

Figure 3. Comparative responses of the $\Delta R/R_0$ versus applied pressure (MPa) for 6, 7, 8, and 9 wt % KB/DPNR nanocomposites (A) and the optimum 6 wt % KB/DPNR nanocomposite (B). [Color figure can be viewed at wileyonlinelibrary.com]

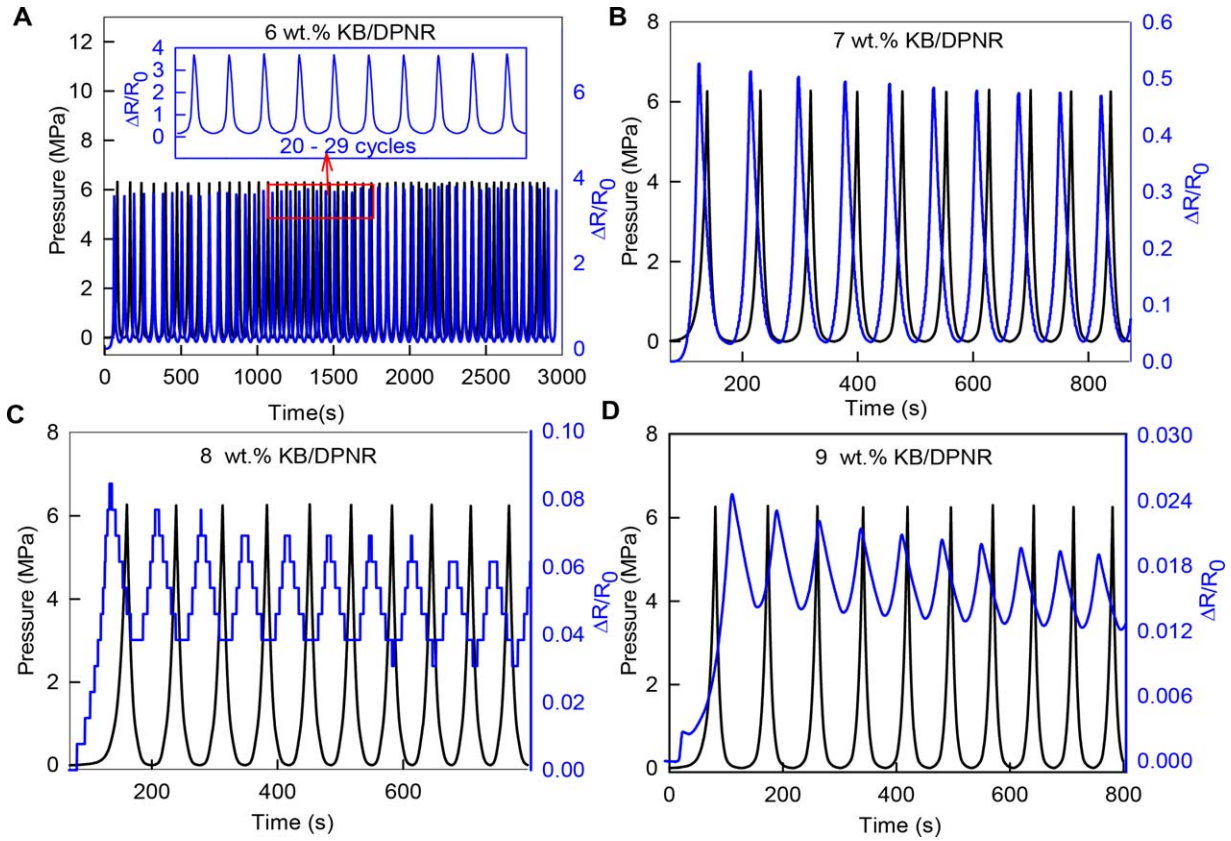

Figure 4. Repeatability of the $\Delta R/R_0$ of 6 wt % KB/DPNR nanocomposite against time (s) for 50 compression cycles induced by 6.25 MPa applied pressure (A) and inset is the enlarged plot of the composites $\Delta R/R_0$ against time from 20 until 29th cycle and 7, 8, 9 wt % KB/DPNR nanocomposites for 10 compression cycles (C,D). [Color figure can be viewed at wileyonlinelibrary.com]

increased resistance during applied pressure indicates that the positive pressure-coefficient effect of resistance (PPCR) occurring in the KB/DPNR throughout the investigated range. This behavior reveals that the KB/DPNR was remarkably suitable for wide range pressure sensing applications compared to the earlier literature on carbon-based composites in the similar range.[2,14–16]

The analysis of piezoresistive responses ($\Delta R/R_0$) of highly sensitive KB/DPNR nanocomposite (6 wt %) under an applied pressure of 12.54 MPa was further carried out. The KB/DPNR showed three transition states in the resistance-pressure curve, as displayed in Figure 3(B). The first transition occurs below the 0.25 MPa (critical region 1), where $\Delta R/R_0$ increased very slowly upon increasing pressure, which reveals that the rate of destruction of the conductive network, is slightly faster than the formation of electrical network [region 1 is zoomed in insert Figure 3(B)]. This observation indicates that the KB may be dragged along with the DPNR chains and pulled apart further which decreases the number of conductive network in the matrix, in agreement with the earlier literature.[24,25] After 0.25 MPa (critical region II), the $\Delta R/R_0$ increased steeply until 3.88 MPa, which indicates that the destruction rate of the electrically conductive network is higher than its formation. This may be due to the matrix initiates to slide along the perpendicular direction of vertically induced pressure, resulting in KB being pulled apart transversely so that the neighbouring KB is further separated and the conductive network is broken. Then, after 3.88 MPa (critical region III), the $\Delta R/R_0$ increased steadily and slowly until 12.54 MPa but the destruction of the network is lesser than region II. This may be due to the reduction of sliding of the matrix and transverse pull of KB along the perpendicular direction of applied pressure.

Repeatability

To examine the repeatability of the $\Delta R/R_0$ of the 6 to 9 wt % KB/DPNR composite, cyclic compressions of 6.25 MPa were carried out for 50 cycles for 6 wt % and 10 cycles for 7 to 9 wt %, as shown in Figure 4(A–D). The results showed that the $\Delta R/R_0$ of 6 and 7 wt % KB/DPNR are highly reversible throughout the investigated cycles and exhibited minimal hysteresis in the first cycle of compression and thereafter negligible hysteresis in the remaining cycles as shown in Figure 4(A,B). Whereas, the 8 and 9 wt % KB/DPNR composite exhibited poor reversibility, reproducibility and higher hysteresis in the investigated 10 cyclic compressive cycles as shown in Figure 4(C,D). These results clearly indicate that the increased KB filler content above 6 wt % might deteriorate the composite performance due to vanishing of tunnelling effect due to the further addition of filler content, in agreement with the earlier literature.[20] The 6 wt % KB/DPNR showed higher $\Delta R/R_0$ (3.76) than the 7 wt % and chosen as an optimum composite for further studies. The 6 wt % KB/DPNR showed consistent $\Delta R/R_0$ values with high repeatability in the investigated 50 cycles, as shown in Figure 4(A).

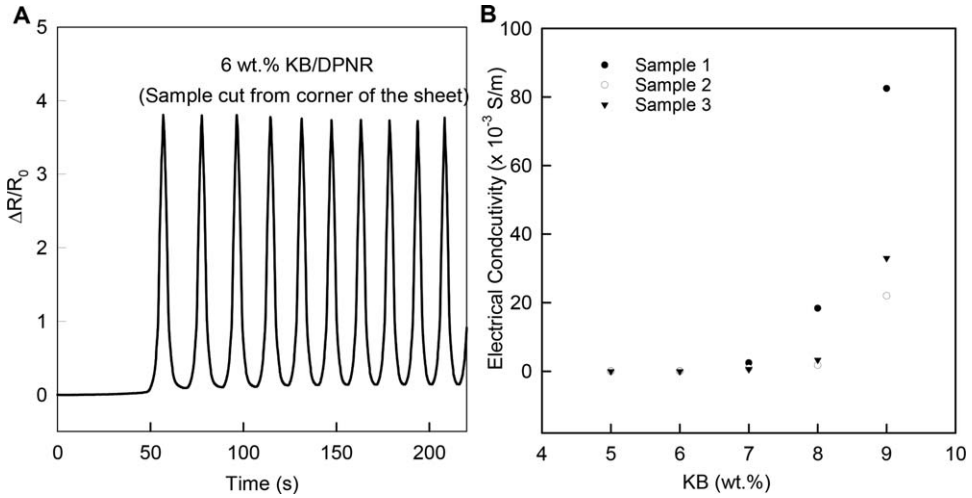

Figure 5. Repeatability of the $\Delta R/R_0$ of the corner portion of 6 wt % KB/DPNR nanocomposite against time (s) for 10 compression cycles induced by 6.25 MPa applied pressure (A) and electrical conductivity (S/m) of 5 to 9 wt % KB/DPNR nanocomposite randomly cut from three portions of the sheet.

The $\Delta R/R_0$ for 20 to 29 cycles is presented in the inset of Figure 4(A). In the first cycle of unloading, the $\Delta R/R_0$ was not completely reversible (difference of $\Delta R/R_0$ is 0.150 from the baseline), which indicates the minimal hysteresis of the developed nanocomposite. However, the second compression cycle has a stabilizing effect on $\Delta R/R_0$ values, which remains same throughout the investigated cycles. To quantify the stability of the $\Delta R/R_0$ responses, the standard deviation (SD) was calculated for both loading and unloading compressive cycles. The SD over 50 loading cycles for peak $\Delta R/R_0$ values was 4.82% of the range 3.56 to 3.76. The SD over the unloading second cycle until 50th cycle for baseline $\Delta R/R_0$ values (range 0.158–0.168) was 3%, which demonstrates that negligible baseline drift was observed from second cycle onwards throughout the cyclic testing. This indicates that during first two cycles of compression, the Ketjenblack may get arranged into the DPNR matrix which stays more or less identical despite the number of compression cycles. The results clearly confirm that the KB/DPNR showed consistent responses to the applied compressive cycles.

Mechanism behind Wide Range Monotonic Piezoresistivity

The unique monotonic piezoresistivity and highest electrical resistance change of 6 wt % KB/DPNR nanocomposite in the wide range of high pressure regime observed in this work may be due to three vital reasons: (i) highly homogeneous dispersion with very low agglomeration of KB within the DPNR matrix, confirmed from the FESEM analysis. This observation is similar to the low carbon nanofiber filler content reinforced natural rubber matrix showing highest dispersion.[21] To further confirm the homogeneous dispersion of the nanocomposite, corner portion of 6 wt % KB/DPNR was cut from the composite sheet and subjected to cyclic compression of 6.25 MPa for 10 cycles under optimal conditions. The corner portion showed excellent reversibility and good repeatability of $\Delta R/R_0$ values [Figure 5(A)] identical to the centre portion of 6 wt % KB/DPNR composite [Figure 4(A)]. A similar study with the horizontally connected electrodes were subjected to piezoresistivity studies for 10 cycles under 6.25 MPa, which resulted in identical repeatability and reversibility (Supporting Information Figure S3) compared to optimal composite. Furthermore, for additional confirmation, three samples were cut randomly from different areas of the 6 wt % KB/DPNR composite sheet and subjected to electrical conductivity measurement. The electrical conductivity results revealed that the 5 and 6 wt % KB/DPNR composite showed very less variation in the conductivity between the three samples than the 7, 8, and 9 wt % KB/DPNR composite, as shown in Figure 5(B) (note: conductivity results of 5 to 9 wt % KB/DPNR are presented in 10^{-3} (S/m) for better graphical representation) and Supporting Information Table S1. All the results indicate that the 6 wt % KB composite exhibited homogeneous dispersion of KB in the DPNR than the higher filler content of KB in the DPNR matrix; (ii) high aspect ratio of the KB which increases the probability of electron transition and more conductive paths between the matrix and KB at a lower filler concentration similar to higher aspect ratio of graphene nanoplatelets tending to lower agglomeration of carbon black within the silicone rubber matrix;[2] and (iii) utilization of double cross linking agent (DCP and SR 350) which leads to enhanced chemical linkages, higher cross linking density, and mechanical properties of KB/DPNR at a lower filler concentration.[26] To confirm the influence of cross linking agents on piezoresistivity of 6 wt % KB/DPNR nanocomposite, the composite was tuned with cross linking agents varied from 0 to 3% as presented in Table II and subjected to cyclic compression of 6.25 MPa for 10 cycles. The $\Delta R/R_0$ of 6 wt % KB/DPNR nanocomposite with and without cross linking agents are shown in Figure 6(A–C). The 6 wt % KB/DPNR with 0% cross linking agents showed nonmonotonic piezoresistivity with decreased $\Delta R/R_0$ and poor repeatability, as shown in Figure 6(A). However, after the incorporation of cross linking agents into the 6 wt % KB/DPNR, the composite exhibited monotonic piezoresistivity regardless to the concentration of cross linking agents as shown in Figures 4(A) and 6 (B,C). In addition, the piezoresistivity of 6 wt % KB/DPNR with 2 and 3 wt % of cross linking agents showed decreased resistance change [Figure 6(B,C)]

Table II. Composition of 6 wt % KB/DPNR Nanocomposites for Varied Cross-Linker's Ratio

		wt % of Ingredients		
Sample no.	DPNR (phr[a])	KB	SR350	DCP
1	100	6	0	0
2	100	6	1.07	1.00
3	100	6	2.14	2.00
4	100	6	3.21	3.00

[a] Part per hundred parts of DPNR by weight.

compared to $\Delta R/R_0$ of KB/DPNR with 1 wt % of cross linking agents [Figure 4(A)] under 6.25 MPa. This result revealed that the cross linking agents might have played a vital role in monotonic piezoresistivity under high pressure along with the homogeneous dispersion and high aspect ratio of KB. The hardness test results revealed that by increasing the wt % of cross linking agents in the 6 wt % KB/DPNR composite, the hardness of the composite increases [Figure 6(D)] in agreement with the earlier literature[26] along with an increase in the resistance values (Supporting Information Table S2). Furthermore, the hardness of the 6 to 9 wt % of KB within the DPNR matrix with 1 wt % cross linking agents is displayed in Supporting Information Table S3, which confirms that the softness (Hardness Shore A 41°) of the 6 wt % KB/DPNR composite is maintained compared to the silicone rubber (Hardness Shore A 40°). Therefore, higher dispersion, more cross linking points, high aspect ratio of KB, and flexibility of 6 wt % KB/DPNR needs greater force for the destruction of the conductive network (i.e., monotonicity is maintained for a wide range of high pressure) in this work.

Sensitivity and Test–Retest Reliability

The piezoresistive response of the 6 wt % KB/DPNR composite was examined at different applied pressure until 12.54 MPa, as shown in Figure 7(A,B). For clarity purposes, the investigated applied pressure range is presented as 0 to 2.49 MPa [Figure 7(A)] and 1.25 to 12.54 MPa [Figure 7(B)]. The KB/DPNR showed highly reversible piezoresistivity with increase in $\Delta R/R_0$

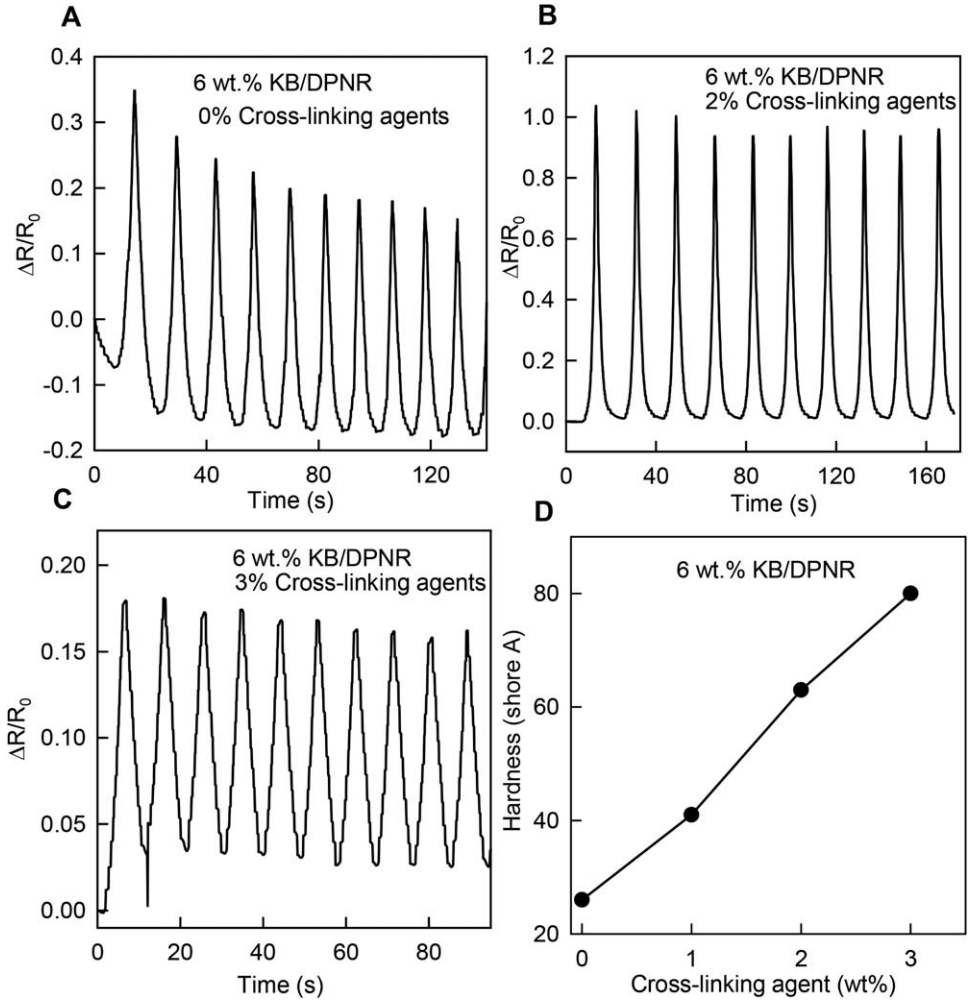

Figure 6. (A–C) Repeatability of the $\Delta R/R_0$ of 6 wt % KB/DPNR nanocomposite against time (s) induced by 6.25 MPa applied pressure with 0, 2, and 3 wt % KB/DPNR nanocomposites for 10 compression cycles and (D) plot of hardness versus varying loadings of cross-linking agents for the 6 wt % KB/DPNR nanocomposite.

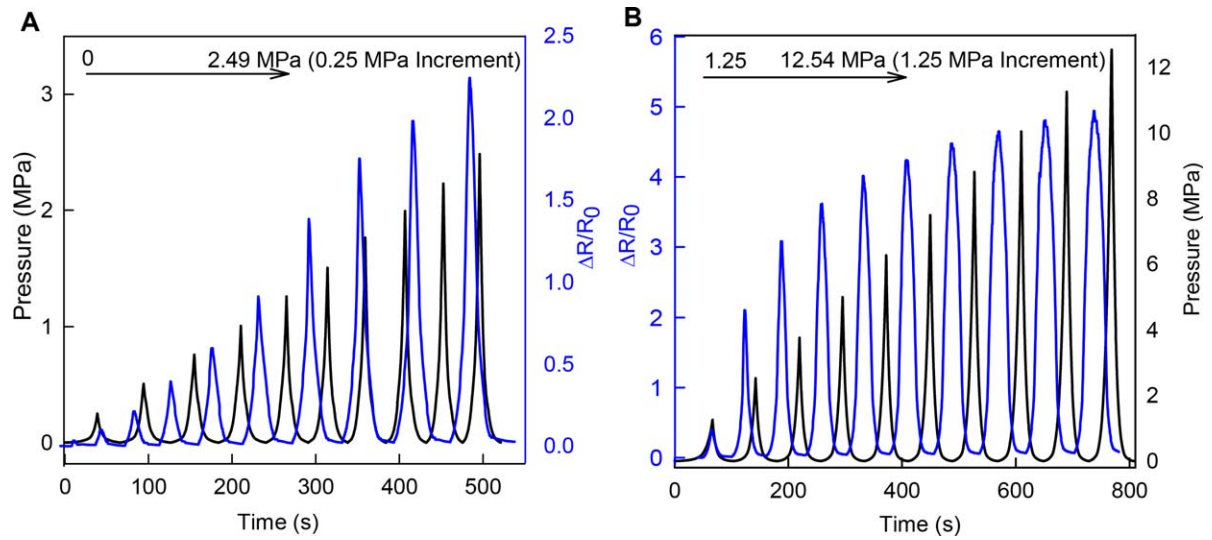

Figure 7. Piezoresistive responses of 6 wt % KB/DPNR versus time (s) for the step increase of applied pressure (0–2.49 MPa) with rise of 0.25 MPa (A) and 1.25 to 12.54 MPa with rise of 1.25 MPa (B). [Color figure can be viewed at wileyonlinelibrary.com]

for increasing pressure throughout the investigated applied pressure regime with minimal hysteresis. In order to demonstrate the optimum KB/DPNR composite as a pressure sensor, the peak point of $\Delta R/R_0$ was plotted against the applied pressure, as shown in Figure 8. The sensitivity (S) was calculated from the slope in the linear region of curve as defined in eq. (2).[10]

$$S = \frac{\delta\left(\frac{\Delta R}{R_o}\right)}{\delta P} \tag{2}$$

where $\Delta R/R_0$ is the relative change in the resistance of the nanocomposite and P is the applied pressure (MPa). The KB/DPNR exhibited linearity in two regions (I and II): Region I exhibited the highest sensitivity (S) = 1.1 MPa^{-1} with good linear regression (Regr = 0.960) in the pressure range of 0.25 to 2.49 MPa.

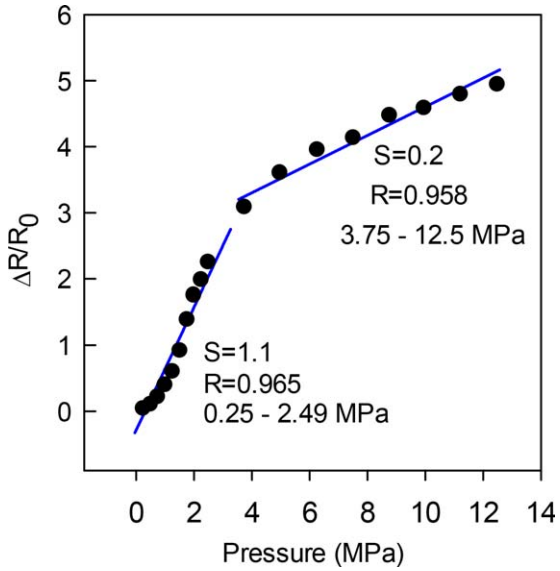

Figure 8. Calibration plot between peak points of $\Delta R/R_0$ of 6 wt % KB/DPNR composite against different applied pressures (MPa). [Color figure can be viewed at wileyonlinelibrary.com]

In the region II, the S exhibited 0.2 MPa^{-1} with a satisfactory linear Regr = 0.958 with a pressure of 3.75 MPa to 12.5 MPa. The results clearly demonstrate that the peak $\Delta R/R_0$ of KB/DPNR gradually reduced with increased applied pressure. The observed trend of KB/DPNR's $\Delta R/R_0$ was similar to the earlier literature on piezoresistive pressure sensor.[10–13,27] Thus, the low-cost, pressure-sensitive KB/DPNR composite exhibited a good sensitivity in the full range of investigated pressure regime in comparison with the other composite reported using other techniques which revealed the sensitivity values of 0.6 kPa^{-1} (0 to 0.3 MPa)[28] and 1.2 MPa^{-1} (0 to 3 MPa) with large hysteresis.[29] This result confirms that the performance of KB/DPNR composite is better than the reported composites in the wide range.

Furthermore, to examine the test–retest reliability of the KB/DPNR's $\Delta R/R_0$, three series of pressure between 0 and 2.49 MPa with an increment of 0.25 MPa were applied on different occasions with an interval of 24 h. The KB/DPNR showed consistent $\Delta R/R_0$ with the same pressure, as shown in Figure 9, which clearly demonstrates the reliable response of the KB/DPNR. To further confirm the test–retest reliability of KB/DPNR's performance, an intra-class coefficient correlation (ICC with 95% confidence interval) was carried out using SPSS statistics software (version 23). To examine the precision and random error of measurements, standard error of measurement (SEM) and coefficient of variance (CV) were calculated using the following formulae[30,31]

$$\text{SEM} = \text{SD of all testing scores} \times \sqrt{}(1 - \text{ICC}) \tag{3}$$

$$\text{CV} = (\text{SD} \times \bar{X})100 \tag{4}$$

where SD is the standard deviation of the repeated measures, the ICC is the coefficient of the reliability, and $\bar{X}$ is the mean of the measurement. All were calculated based on the peak responses with pressure on three repeated measurements. The obtained ICC was 0.998 for three $\Delta R/R_0$ measurements which indicates the excellent reliability of the KB/DPNR's performance for three repetitions. The SD for the three $\Delta R/R_0$ measurements

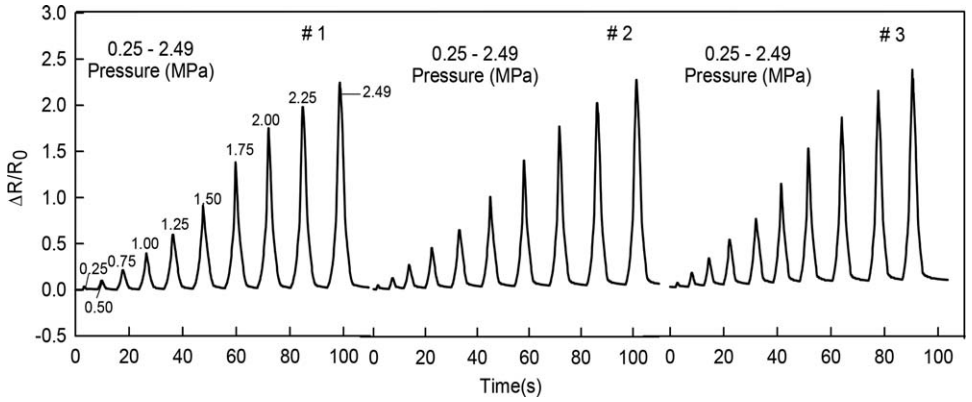

Figure 9. Test–retest reliability of $\Delta R/R_0$ response of the 6 wt % KB/DPNR composite against time for the applied pressure from 0 to 2.49 MPa with rise of 0.25 MPa on three different occasions at an interval of 24 h.

was less than 5% of all pressure except 1.50 MPa. The lowest SD of 0.4131 for 0.25 MPa and highest SD of 6.5283 for 1.50 MPa were observed. The calculated CV % and SEM % for the three repeated measurements (0–2.49 MPa) are given in the Supporting Information Table S4. The obtained results of CV and SEM were less than 7% and 1%, respectively. A CV % (<10) and SEM % (<3.5) were considered as an acceptable range of random error of measurement and high precision of measurement, respectively.[30,31] These statistical results (ICC = 0.99, CV < 7%, and SEM < 1%) revealed that the performance of KB/DPNR is remarkably excellent in terms of test–retest reliability with minimum random error and high precision of measurement.

Conditioning and Calibration of KB/DPNR Composite for Real-Time Monitoring

To demonstrate the real-time monitoring of pressure sensing applications, the optimum KB/DPNR composite ($R_4 = 8.68$ MΩ) was integrated with a Wheatstone bridge ($R_1 = 9.98$ KΩ, $R_2 = 9.98$ KΩ, $R_3 = 0$–10 MΩ) with low excitation voltage supply (3 V), signal conditioning circuit (R–C conversion), microcontroller (ATMEGA 328) controlled by a custom-built Simulink program, and PC. The output voltage of the bridge was amplified (amplification factor of 500) and filtered using a low pass filter (31.53 Hz). The low pass filter was designed using eq. (5).[32,33]

$$F_c = \frac{1}{2\pi RC} \tag{5}$$

where F_c is the cutoff frequency, R is resistor (504.89 Ω), and C is the capacitor (10 μF). The sampling frequency of the device was set at 200 Hz to avoid the loss of data during testing.

The KB/DPNR composite was conditioning and calibrated with standard loads before subjecting it to real time testing. Initially, the composite was conditioned to compression loads of 30 kg (three times greater than the expected pressure) through several loading and unloading cycles. The resistance and voltage of the composite were measured before and after testing with loading and unloading cycles. Initially, the bridge was balanced and the measured resistance of the sensor was 8.64 MΩ. After unloading, the output voltage and resistance were found to settle at 29 mV and 9.73 MΩ, respectively.

The resulting output voltage (29 mV) of the device was then taken as a baseline value for calibration testing. Then, the known static compressive load (0.24–2.42 MPa) with the increment of 0.24 MPa was applied several times in the active area of the composite and maintained for a few seconds until a steady output was observed.[34] The device responses showed significant change in voltage output with each 0.24 MPa increment, as shown in Figure 10, which indicates the suitability of the system in this working range. In addition, the linearity of the developed device was established by plotting the peak point of the voltage response against the compressive load, as shown in the inset of Figure 10. The device exhibited excellent linearity (Regr = 0.987) in the investigated range of 0 to 2.42 MPa.

Real-Time Measurement

Finger Pressure. To confirm the suitability of the developed system for real-time finger pressure sensing applications, the finger pressure was applied by a researcher for 75 times over the centre portion of the KB/DPNR composite with 30 s rest

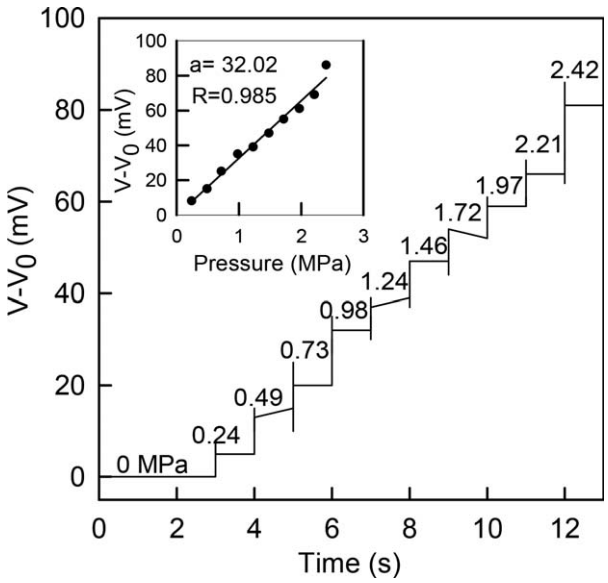

Figure 10. (A) Voltage response of the developed device (mV) under static load (0–2.42 MPa) with step increase of compressive load of 0.24 MPa versus time (s) and inset is its respective calibration plot.

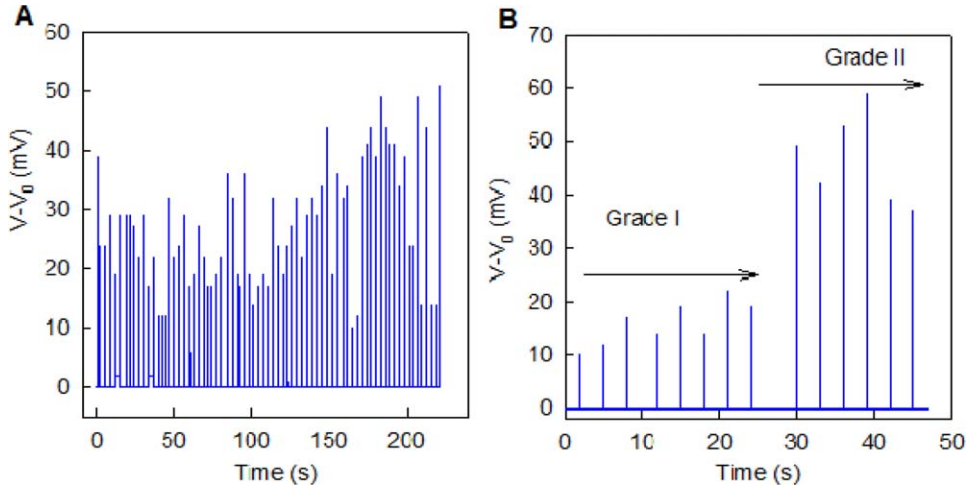

Figure 11. Real-time response of the developed system (mV) versus time (s) for applied finger pressure of 75 times (A) and bone movement (grade I and II) performed through finger pressure on human (B). [Color figure can be viewed at wileyonlinelibrary.com]

given between each applied pressure to minimize the muscle fatigue of the subject during testing. The performance of the developed system to the applied finger pressure (mV) versus time (s) is shown in Figure 11(A). This result confirms that the developed system is suitable for real-time finger pressure measurements.

Pressure Monitoring during Bone Movement. To demonstrate the potential real-life application of the developed system, 30-year-old male suffering with spinal pain was recruited. The patient was informed about the study procedure and obtained the informed consent before participating in the study. Before performing accessory movement of bone i.e., joint mobilization treatment, the KB/DPNR composite was positioned over the transverse process of lumbar vertebra (L). Then, the grade I and II accessory movement of bone over the L4 and L5 were performed by clinician for eight times by applying finger pressure over the active area of the composite. The results of performance of the developed system against the finger pressure (mV) versus time (s) are shown in Figure 11(B) and Supporting Information Figure S4. The developed system showed excellent response depending upon the amount of pressure exerted on it. All these results collectively confirm that the KB/DPNR composite is highly sensitive and reliable for finger pressure monitoring applications.

CONCLUSIONS

Our work on the piezoresistivity of the KB/DPNR nanocomposite under applied compressive pressure (0–12.54 MPa) and the integration of KB/DPNR with the microcontroller leads to the following conclusions: (1) a monotonic positive piezoresistive behavior of the novel KB/DPNR nanocomposite under wide pressure range (0–12.54 MPa) was achieved. (2) The 6 wt % KB/DPNR nanocomposite exhibited the highest electrical resistance change (485%) with remarkable reversible piezoresistivity, good sensitivity, excellent test–retest reliability, and repeatability with minimal hysteresis under a wide range of compressive load compared to earlier literature. This may be due to homogenous dispersion, high aspect ratio of KB, enhanced chemical linkage, and high cross linking density between KB and DPNR. (3) The KB/DPNR nanocomposite was successfully tested for real time monitoring of finger pressure. Further, accessory movement of bone (grade I and grade II) were demonstrated on a subject with a spinal pain using the developed system in real life situations for the first time.

ACKNOWLEDGMENTS

J.M. thanks Sakura Rubber Sdn.Bhd, Penang, Malaysia, for the two-roll mill facility provided. The authors thank Fadili, Material Testing laboratory for the technical help rendered during electromechanical testing. The materials testing laboratory and central analysis unit facilities provided by the Mechanical Engineering and Biosciences and Medical Engineering Faculties, UTM are sincerely acknowledged. J.M. thanks UTM for the International Doctoral Fellowship awarded.

REFERENCES

1. Tiwana, M. I.; Redmond, S. J.; Lovell, N. H. *Sens. Actuators A* **2012**, *179*, 31.
2. Cai, W.; Huang, Y.; Wang, D.; Liu, C.; Zhang, Y. *J. Appl. Polym. Sci.* **2014**, *131*, DOI: 10.1002/app.39778.
3. Yamada, T.; Hayamizu, Y.; Yamamoto, Y.; Yomogida, Y.; Izadi-Najafabadi, A.; Futaba, D. N.; Hata, K. *Nat. Nanotechnol.* **2011**, *6*, 296.
4. Wang, Y.; Yang, R.; Shi, Z.; Zhang, L.; Shi, D.; Wang, E.; Zhang, G. *ACS Nano* **2011**, *5*, 3645.
5. Zheng, W.; Wong, S. C. *Compos. Sci. Technol.* **2003**, *63*, 225.
6. Wang, P.; Ding, T. *J. Appl. Polym. Sci.* **2010**, *116*, 2035.
7. Das, N. C.; Maiti, S. *J. Mater. Sci.* **2008**, *43*, 1920.
8. Dubnikova, I.; Kuvardina, E.; Krasheninnikov, V.; Lomakin, S.; Tchmutin, I.; Kuznetsov, S. *J. Appl. Polym. Sci.* **2010**, *117*, 259.
9. Raza, A. M.; Westwood, A.; Stirling, C.; Brydson, R.; Hondow, N. *J. Appl. Polym. Sci.* **2012**, *126*, 641.

10. Tai, Y.; Mulle, M.; Ventura, I. A.; Lubineau, G. *Nanoscale* **2015**, *7*, 14766.
11. Tian, H.; Shu, Y.; Wang, X. F.; Mohammad, M. A.; Bie, Z.; Xie, Q. Y.; Li, C.; Mi, W. T.; Yang, Y.; Ren, T. L. *Sci. Rep.* **2015**, *5*, 8603.
12. Boland, C. S.; Khan, U.; Backes, C.; O'Neill, A.; McCauley, J.; Duane, S.; Shankar, R.; Liu, Y.; Jurewicz, I.; Dalton, A. B.; Coleman, J. N. *ACS Nano* **2014**, *8*, 8819.
13. Hou, Y.; Wang, D.; Zhang, X. M.; Zhao, H.; Zha, J. W.; Dang, Z. M. *J. Mater. Chem. C* **2013**, *1*, 515.
14. Wang, L.; Wang, X.; Li, Y. *Compos. A* **2012**, *43*, 268.
15. Yoshimuraa, K.; Nakanoa, K.; Okamotoa, K.; Miyakeb, T. *Sens. Actuators A* **2012**, *180*, 55.
16. Lu, J.; Weng, W.; Chen, X.; Wu, D.; Wu, C.; Chen, G. *Adv. Funct. Mater.* **2005**, *15*, 1358.
17. Pichayakorn, W.; Suksaeree, J.; Boonme, P.; Taweepreda, W.; Ritthidej, G. C. *Ind. Eng. Chem. Res.* **2012**, *51*, 13393.
18. Tanaka, Y.; Sakadapipanich, J. U.S. Pat. 7,687,602B2 (**2010**).
19. Rattanasom, N.; Thammasiripong, U.; Suchiva, K. *J. Appl. Polym. Sci.* **2005**, *97*, 1139.
20. Souri, H.; Nam, I. W.; Lee, H. K. *Compos. Sci. Technol.* **2015**, *121*, 41.
21. Abraham, E.; Deepa, B.; Pothan, L. A.; John, M.; Narine, S. S.; Thomas, S.; Anandjiwala, R. *Cellulose* **2013**, *20*, 417.
22. Barbara, S. Infrared Spectroscopy: Fundamentals and Applications; John Wiley and Sons Ltd., England **2004**; p 139.
23. Peter, M. Carbon Fibers and their Composites; Taylors and Francis, Florida, **2005**; Chapter 1, p 12.
24. Chen, L.; Chen, G.; Lu, L. *Adv. Funct. Mater.* **2007**, *17*, 898.
25. Knite, M.; Teteris, V.; Kiploka, A.; Kaupuzs, J. *Sens. Actuators A* **2004**, *110*, 142.
26. Shao, L.; Ji, Z. Y.; Ma, J. Z.; Xue, C. H.; Ma, Z. -L.; Zhang, J. *Sci. Rep.* **2016**, *6*, 36931.
27. Yao, H. B.; Ge, J.; Wang, C. F.; Wang, X.; Hu, W.; Zheng, Z. J.; Ni, Y.; Yu, S. H. *Adv. Mater.* **2013**, *25*, 6691.
28. Zhao, H.; Bai, J. *ACS Appl. Mater. Interfaces* **2015**, *7*, 9652.
29. S. L. Wang, S. L.; Wang, P.; Ding, T. H. *Sens. Actuators A* **2010**, *157*, 36.
30. Yu, W. H.; Chen, K. L.; Huang, S. L.; Lu, W. S.; Lee, S. C.; Hsieh, C. L. *Arch. Phys. Med. Rehabil.* **2016**, *97*, 2137.
31. Paungmali, A.; Sitilertpisan, P.; Taneyhill, K.; Pirunsan, U.; Uthaikhup, S. *Asian J. Sports Med.* **2012**, *3*, 8.
32. Singh, O. P.; Mekonnen, D.; Malarvili, M. B. *J. Med. Eng.* **2015**, Article ID 701520, 9 pages.
33. Kang, I.; Schulz, M. J.; Kim, J. H.; Shanov, V.; Shi, D. *Smart Mater. Struct.* **2006**, *15*, 737.
34. Noce, H. P. Master Thesis, Oregon State University, USA, **2005**.